Published in final edited form as:
Langmuir. 2010 June 1; 26(11): 8684–8689. doi:10.1021/la904842v.

Studies of Bilayers and Vesicle Adsorption to Solid Substrates: Development of A Miniature Streaming Potential Apparatus (SPA)

Younjin Min[†], **Noshir Pesika**[‡], **Joe Zasadzinski**[†,*], and **Jacob Israelachvili**[†,*]

[†]Department of Chemical Engineering, University of California Santa Barbara, Santa Barbara, CA 93106, USA

[‡]Department of Chemical and Biomolecular Engineering, Tulane University, New Orleans LA 70118, USA

Abstract

A new miniature streaming potential apparatus (SPA) was developed to determine the streaming potentials (Ψ_{str}) and zeta potentials (ζ) of substrates under different ionic conditions while simultaneously visualizing the state of the surfaces, such as the adsorption of surfactants or polymers, using fluorescence microscopy and/or fluorescence recovery after photobleaching (FRAP). Experimental results with different surfaces show that the new SPA provides streaming potential values (hence zeta potentials) that agree with results obtained using traditional electrokinetic analyzers. Using the new SPA, the formation of supported lipid bilayers (SLBs) on glass from fluorescently labeled, unilamellar (~100 nm diameter), charge neutral dimyristoyl-*sn*-glycero-3-phosphocholine (DMPC) vesicles was studied in aqueous electrolyte solutions at different lipid concentrations. Simultaneous zeta potential measurements and fluorescence imaging for measuring diffusion coefficients by confocal microscopy enabled us to precisely monitor the changes in the surface charge as well as in the surface morphology during SLB formation from vesicles. For a fixed incubation time of 5 minutes, both results revealed that the adsorption of intact vesicles and/or discrete bilayer patches were observed below a threshold concentration, above which the formation of continuous SLBs occurred leading to an estimate for the ζ-potential and for the diffusion coefficient of -9.1 ± 1.6 mV and $(1.1\pm0.02)\times10^{-12}$ m^2/s, respectively.

1. Introduction

Supported lipid bilayers (SLBs) have been extensively studied as models of cellular membranes for certain biophysical phenomena such as cell-cell interactions,[1–4] and as building blocks for biomedical applications such as biosensors.[2,5–7] Vesicle fusion for SLB formation is one of the most convenient ways to provide large scale robust bilayers since it does not require sophisticated equipment and allows the deposition of membranes with proteins[3] or specific functional groups for chemical sensing.[8]

Despite the scientific importance and practical convenience of vesicle fusion onto substrates, the mechanisms and kinetics of the formation of well-controlled continuous supported bilayers are still not fully understood. A number of studies have identified some of the critical stages of vesicle adsorption (adhesion), fusion, deformation, rupture, and spreading in the formation process.[9–12] However, the interactions between vesicles and substrates during their collisions [13,14] across a thin water layer approximately 1–2 nm thick [15,16] and the mechanisms of their adsorption and transformation into SLBs remain to be explored in more detail.

*To whom correspondence should be addressed. gorilla@engineering.ucsb.edu and jacob@engineering.ucsb.edu.

Ions in the aqueous medium play a very crucial role in the formation of SLBs from vesicles. They affect both the electrostatic and osmotic stresses[9,13,17,18] within vesicles, and the forces between them and the solid surfaces that lead to adhesion and rupture, followed by the fusion of the fragments into a single continuous bilayer on the surface.[10,19–22] A variety of techniques have been used to investigate SLB formation processes including atomic force microscopy (AFM),[10,23–25] quartz-crystal microbalance (QCM),[26–29] fluorescence microscopy,[11,30] ellipsometry,[31,32] surface plasmon resonance (SPR),[27] interference contrast microscopy,[9,33]; but none of these techniques have focused on the subtle but important electrochemical changes associated with SLB formation.

From an experimental point of view, the streaming potential (Ψ_{str}) technique can be used to determine the zeta potentials (ζ) and other electrostatic characteristics of a membrane surface.[34,35] The streaming potential technique, initially developed by Van Wagenen and Andrade,[36] has become a common tool for measuring ζ because of its versatility, for example, allowing for large macroscopic surfaces to be used. However, to our knowledge, no study has quantified the dynamic changes in ζ potential during SLB formation. With the aim of establishing and correlating the electrostatic interactions during the various stages of the formation of SLBs of uncharged lipids from vesicles with their diffusion in the bilayers, a new miniature streaming potential apparatus (SPA) was developed (Figure 1).

2. Experimental Section

Streaming potential apparatus (SPA)

A new miniature SPA (Figure 1) was developed to simultaneously measure surface potentials and record fluorescence images of the surfaces. The size of the 'miniature' SPA was kept small so that the entire unit could be placed on the translational stage of a confocal microscope or other optical microscope. The small size and volume also benefit studies in which only small quantities of materials are available. The cell in the SPA consists of a thin channel formed by two flat solid surfaces – a 'reference' Teflon surface and a transparent (glass) surface, with an inlet and an outlet compartment at each end. The parallel plate channel 12 mm long (l) × 7 mm wide (w) × 0.08 mm high (h) was constructed by clamping the two surfaces together while separated by a Teflon piece providing a ~80 μm gap between the surfaces. An injection point in the side wall was used to introduce the vesicle solution and also to record the solution temperature using a thermocouple. All stainless steel parts (SS 316) were periodically disassembled, passivated in nitric acid solution (30% *v*/*v*) at 60°C for 30 min, thoroughly rinsed with distilled water and then cleaned with chloroform and ethanol before use. The passivation creates an impermeable metal oxide layer on the 316 stainless steel surface that prevents the leaching of metal ions into the buffer solution during experiments. Borosilicate glass (Fisher Scientific Inc., CA) was cleaned with ethanol and treated with UV-Ozone (UVOCS Inc., PA) for 30 min. Teflon parts were cleaned with chloroform before use. Two different sets of substrates, Teflon against borosilicate and Teflon against Teflon, under different buffer solution concentrations (1, 10, and 100 mM KCl solutions) were used to validate the new SPA.

Preparation of vesicle solutions

Zwitterionic lipid dimyristoyl-*sn*-glycero-3-phosphocholine (DMPC) (Avanti Polar Lipids, AL) and Texas Red® 1,2-dihexadecanoyl-*sn*-glycero-3-phosphoethanolamine, triethylammonium (TR-DHPE) (Molecular Probes, OR) which has excitation and emission at 596 and 615 nm, respectively, were used to prepare the vesicle solutions. All lipids were stored at −20°C until used. The preparation of DMPC vesicles containing 1 wt% TR-DHPE were carried out by the extrusion method.[37,38] Briefly, DMPC and TR-DHPE lipids were dissolved and mixed in chloroform, then dried by gently purging with nitrogen gas, kept under vacuum overnight to remove the residual chloroform, and then stored in a vacuum desiccator until ready

for use. Dry DMPC and TR-DHPE film were rehydrated in 100 mM KCl (ACS grade, Sigma-Aldrich Co., MO) at a concentration of 1 mg/ml, after which the solution was subjected to ten freeze-thaw cycles consisting of freezing the solution in liquid nitrogen followed by submersion in a water bath (Fisher Scientific Inc., CA) at 45°C, which is above the main chain transition temperature ($T_m \approx 24$ °C) of DMPC. The resulting vesicle solution was then extruded ten times, first through polycarbonate membranes (SPI Supplies Division Structure Probe Inc., PA) of pore diameter 200 nm followed by membranes of pore diameter of 100 nm. The extrusion was carried out by standard extrusion methods using a Lipex Biomembranes Extruder (Vancouver, Canada) in a home-built setup to achieve constant pressure during the extrusion, and care was taken to ensure that the extrusion took place above the T_m of DMPC using a water bath.

Vesicle size and ζ-potential measurements of the vesicles in solution were performed by a Zetasizer 3000HS electrophoresis analyzer (Malvern Instruments Ltd., UK) and found to have a mean diameter of 111±1 nm with a very narrow polydispersity index (PDI) of 0.05±0.02. The ζ-potential of the vesicles were slightly negative (−1.74±0.70 mV) in 100 mM KCl buffer solution. The vesicles appeared to be stable in the buffer solution and were stored at 4 °C until used. Milli-Q water was used in all experiments and was purified by a MilliPore Gradient A10 system (Millipore Corporate, MA) resulting in dionized water with a resistivity of ≥18.2 MΩ·cm and total organic content of ≤5 ppb. The vesicle solution was diluted to 0.1 mg/ml prior to the streaming potential and fluorescence recovery after photobleaching (FRAP) measurements.

Streaming potential measurements with vesicle solutions

The streaming potential across an electrolyte solution flowing through the cell under a regulated and constant hydrostatic pressure provided by a syringe pump (Harvard Apparatus, MA) was measured by two Ag/AgCl electrodes (Bioanalytical systems Inc., IN), one in each compartment, connected to an electrometer (Model 6514 Programmable Electrometer, Keithley Instruments, Inc., OH). Flow rates, Q_R, were carefully calibrated before experiments and then converted to the corresponding pressure drop, ΔP, based on the appropriate hydrodynamic equation for a rectangular geometry:[39]

$$Q_R \approx \frac{wh^3 \Delta P}{12\eta l}, \tag{1}$$

where w is the width, h is the height, l is the length of the channel, and η is the viscosity of the medium which is 0.001 Pa·s. For each measurement of zeta potential ζ, a series of streaming potential measurements Ψ_{str} were done at five or more different pressures P to obtain the slope $\Delta\Psi_{str}/\Delta P$. The slope was converted to the zeta potential ζ using the Helmholtz-Smoluchowski (H-S) equation:[34,39]

$$\frac{\Delta\Psi_{str}}{\Delta P} = \frac{\varepsilon_o \varepsilon_r \zeta}{\eta\lambda}, \tag{2a}$$

where ζ is the zeta potential of surface and where ε_o and ε_r are the permittivity of free space and the relative permittivity of the medium, respectively. For dissimilar surfaces, the modified H-S is used:[40]

$$\frac{\Delta\Psi_{str}}{\Delta P} = \frac{\varepsilon_o \varepsilon_r}{\eta\lambda}\frac{(\zeta_{Top} + \zeta_{Bottom})}{2} = \frac{\varepsilon_o \varepsilon_r \zeta_{average}}{\eta\lambda}, \tag{2b}$$

where $\zeta_{average}$ is the average zeta potential of the top (ζ_{Top}) and bottom (ζ_{Bottom}) surfaces (see Fig. 2 (c)). The conductivity of the medium, λ, was measured using a YSI 3200 Conductivity Instrument (Cole-Parmer, IL) and found to be 0.015±0.002 $\Omega^{-1}\cdot m^{-1}$ for 1 mM, 0.14±0.02 $\Omega^{-1}\cdot m^{-1}$ for 10 mM, and 1.3±0.1 $\Omega^{-1}\cdot m^{-1}$ for 100 mM KCl buffer solutions. To ascertain the cleanliness of the substrates, streaming potentials were measured on the bare surfaces using buffer solutions with the same ionic strengths as the vesicle solutions to be injected later. The outlet of the SPA was connected to a syringe containing the same buffer solution, and the injection point (see Fig. 1) was uncapped to prepare the injection of the bulk DMPC vesicle solution.

Different volumes of a bulk DMPC vesicle solution (0.1 mg/ml in buffer) were then injected through the injection point by pulling out a comparable volume of buffer solution with the syringe through the outlet to make sure no air bubbles were introduced into the SPA during this process. The vesicles were distributed through the entire chamber by passing ~1.5 times the volume of the inlet compartment through the SPA (~50 times the channel volume) at which point the dye color could be seen to come out from the outlet. The flow was then stopped and the chamber allowed to incubate, undisturbed, for 5 min at room temperature.

Excess vesicles which did not adsorb on the surfaces were then removed from the cell by flushing (rinsing) with pure buffer. This rinsing was done to eliminate the background fluorescence signal from the unadsorbed vesicles. A confocal microscope (Nikon C1 plus, Nikon Instruments Inc., NY) equipped with a HeNe laser and 20× objective was used for optical imaging and the FRAP experiments. To probe the continuity and fluidity of the bilayer, a spot approximately 7.5 μm in diameter was illuminated with an intense He/Ne laser for 10 sec to bleach the fluorescent lipid molecules in the beam line. Images were collected intermittently under wide-field attenuated illumination to monitor the fluorescence recovery of the darkened spot. During all the measurements, the SPA was clamped on the stage of the microscope, and the temperature of the SPA and electrolyte solution was maintained at 22.5±0.5 °C. The diffusion coefficient D of the lipids was obtained using a previously reported method.[41,42] Briefly, plotting $a^2/2$ *vs*. time t for a series of intensity profiles obtained from images taken during the recovery process gives the diffusion coefficient where a represents the full width at half maximum of the cross-sectional fluorescence intensity profile obtained by a Gaussian fitting procedure.

3. Results and discussion

In order to verify the performance of the miniature SPA, the electrokinetic characteristics of bare (i) Teflon versus Teflon, and (ii) Teflon versus borosilicate substrates were measured in C = 1, 10, and 100 mM KCl solutions. Figure 2 shows our results which are in good agreement with previous measurements43,[44] based on a modified Helmholtz-Smoluchowski (H-S) equation.[40] An interesting finding is the exponential relationship between C with ζ: [44]

$$\zeta = b \ln C + const., \tag{3}$$

where b is a constant given by b = 5.6 mV in Fig. 2(a) and b = 14.0 mV in Fig. 2(b). This exponential dependence has been previously observed and discussed for high ζ values,[45] where typical values measured were in the range 12–30 mV,[44] which may be compared with the electrochemical constant of $kT/e \approx 26$ mV at 295K.

Different amounts of DMPC vesicle solutions were introduced into the SPA chamber to visualize and quantify (through the ζ potential values) the stages the vesicles go through as they adsorb (adhere), rupture and ultimately fuse to form a uniform bilayer on a borosilicate

surface. We define the dimensionless number ***N*** in Fig. 3 as the total number (mass) of DMPC molecules in the SPA chamber during the incubation/adsorption period (see Experimental section), normalized by the number of molecules needed to form a continuous bilayer (SLB) on the glass and a monolayer on the Teflon surfaces. The actual concentrations of vesicles in the SPA chamber, $C_{vesicle}$, varied from 0.001 mg/ml to 0.1 mg/ml as shown in Fig. 4. Stage I is defined by the lack of fluorescence recovery after photobleaching, while Stage II is defined by the visual observation of full fluorescence recovery within at the most 60 seconds after photobleaching (see Fig. 5). The fluorescence images show that the initial adhesion process proceeded slowly even when $14 \geq N > 0$ (Stage I) indicating that there were only vesicles and/or patchy bilayers at this stage. Since during Stage I there are already excess DMPC lipid molecules ($N > 1$), this means that not every vesicle-surface collision results in adhesion or adsorption. However, when $N \geq 22$ (Stage II), the glass surface is uniformly (evenly) fluorescent and is presumably completely covered by a continuous DMPC bilayers (Fig. 3).

Simultaneous ζ-potential measurements were made during the imaging. As shown in Fig. 4, only small increases in the ζ-potential values were observed during Stage I, while there was a large and abrupt increase in the ζ-potential when $N \geq 22$, consistent with the formation of a complete bilayer as found in the fluorescence images (Fig. 3). Our observations are consistent with previous work where it was found that vesicles are stable on a glass surface until a "threshold density" is reached, at which point there is a rapid conversion of adsorbed vesicles or bilayer patches into SLBs.[21,26,31,46] For example, the clear signs on the formation of a defect free PC bilayers directly from vesicle solution have been observed at or above 0.1 mg/ml lipid concentration based on the QCM[26] and FRAP[46] results after a fixed incubation time of ≤5min which strongly agree with our conclusions using the new SPA (Fig. 4). Our results also suggest that in order to obtain a continuous lipid bilayer (or enter Stage II), the initial bulk concentration of the lipids has to be above a threshold concentration (0.036 ml/ml of vesicles in buffer solution). We do not observe the formation of a continuous bilayer by the incremental addition of lipids even beyond $N = 22$ (see open circles in Fig. 4). Once the formation of a bilayer is complete (for $N \geq 22$), there is no further significant change in the fluorescence and the ζ-potential.

The ability of the adsorbed DMPC lipids to diffuse laterally in the plane of the surface (surface diffusion) was also investigated by fluorescence recovery after photobleaching (FRAP), as illustrated in Fig. 5. If the DMPC vesicles remain intact as individual vesicles and/or patchy bilayers, as observed during Stage I, there should be no long range diffusion and therefore no recovery after photobleaching. On the other hand, once the adsorbed vesicles or patches fuse to form a SLB, the DMPC lipids should be fully laterally mobile within the SLB. The measured lateral diffusion coefficients, *D*, of DMPC bilayers on the borosilicate glass in 100 mM KCl buffer solution were in the range of 10^{-12} m^2/s, depending on the vesicle concentration, which are in good agreement with literature values.[47]

Figure 6 shows plots of the ζ-potentials and diffusion coefficients *D* of a DMPC-covered surface as a function of vesicle concentration ***N***, 10 min after vesicle solution injection. The results are consistent with the previously shown data, as well as with the observations by Keller *et al*.[27] that a critical vesicle coverage is required to trigger and/or cause continuous bilayers to form. The abrupt change in the adsorption dynamics above some critical vesicle concentration (around $N = 20$ in our studies) is shown by the dashed vertical line in Fig. 6.

The formation of a SLB causes an abrupt change in the (negative) surface potential from −40 to −10 mV. Interestingly, we obtain a negative ζ-potential of −9.1±1.6 mV at the end of Stage II where a continuous bilayer is presumably covering the surface even though DMPC is zwitterionic and therefore uncharged. However, for the glass-bilayer interface to have zero charge, the negatively charged glass surface must also be neutralized by the K^+ counterions in

the solution. It is clear that some of the counterions in the double-layer remain trapped between the surfaces as the neutral DMPC bilayer adsorbs to it owing to the surfaces interacting between "constant potential" and "constant charge".[46]

4. Conclusions

We described the design and performance of a miniature streaming potential apparatus (SPA) that can be mounted on a microscope stage. The SPA was tested with two sets of substrates and streaming potential values (hence ζ-potential values) which were in good agreement with previous measurements for both similar (Teflon *vs.* Teflon) and dissimilar (Teflon *vs.* glass) surfaces. The small volume and portability of this SPA makes it suitable for imaging biological and non-biological structures in solution and on surfaces under well-controlled solution, electric field and flow conditions.

For the bilayer system studied here (DMPC bilayer-covered borosilicate glass surfaces), the SPA allowed simultaneous visual fluorescence imaging with ζ-potential and FRAP diffusion measurements. The results show a two-step process for the formation of DMPC bilayers on a borosilicate surface from vesicles in the solution: at low concentrations, adsorbed vesicles do not spread (or spread very slowly) and the ζ-potential hardly changes. Above a certain critical concentration there is rapid rupture and fusion of the bilayer fragments into a single continuous bilayer (SLB) during which the ζ-potential drops rapidly to a low value. The later indicates that some of the counterions in the diffuse double-layer remain trapped between the neutral bilayer and (negatively charged) glass surface. This is suggestive of a 'charge-regulated' bilayer-glass double-layer interaction intermediate between constant potential and constant charge.

Acknowledgments

This work was supported by NIH grant R01 GM076709 and was also partially supported by the Materials Research Laboratory Program of the National Science Foundation under Award DMR00-80034, National Institutes of Health Grant HL-51177.

References

1. Watts TH, Gaub HE, McConnell HM. Nature 1986;320:179–181. [PubMed: 2936964]
2. Sackmann E. Science 1996;271:43–48. [PubMed: 8539599]
3. Salafsky J, Groves JT, Boxer SG. Biochemistry 1996;35:14773–14781. [PubMed: 8942639]
4. Reviakine I, Bergsma-Schutter W, Brisson A. Journal of Structural Biology 1998;121:356–362. [PubMed: 9705879]
5. Groves JT, Boxer SG. Accounts of Chemical Research 2002;35:149–157. [PubMed: 11900518]
6. Boxer SG. Current Opinion in Chemical Biology 2000;4:704–709. [PubMed: 11102877]
7. Kam L, Boxer SG. Langmuir 2003;19:1624–1631.
8. Hook F, Ray A, Norden B, Kasemo B. Langmuir 2001;17:8305–8312.
9. Radler J, Strey H, Sackmann E. Langmuir 1995;11:4539–4548.
10. Reviakine I, Brisson A. Langmuir 2000;16:1806–1815.
11. Johnson JM, Ha T, Chu S, Boxer SG. Biophysical Journal 2002;83:3371–3379. [PubMed: 12496104]
12. Weirich KL, Fygenson D, Israelachvili J. Biophysical Journal. 2009
13. Israelachvili, JN. Intermolecular and Surface Forces. Second Edition ed.. Academic Press; 1991.
14. Parsegian VA. Langmuir 1993;9:3625–3628.
15. Johnson SJ, Bayerl TM, McDermott DC, Adam GW, Rennie AR, Thomas RK, Sackmann E. Biophysical Journal 1991;59:289–294. [PubMed: 2009353]
16. Koenig BW, Kruger S, Orts WJ, Majkrzak CF, Berk NF, Silverton JV, Gawrisch K. Langmuir 1996;12:1343–1350.

17. Nollert P, Kiefer H, Jahnig F. Biophysical Journal 1995;69:1447–1455. [PubMed: 8534815]
18. Cha T, Guo A, Zhu XY. Biophysical Journal 2006;90:1270–1274. [PubMed: 16449198]
19. Seifert U, Lipowsky R. Physical Review A 1990;42:4768–4771. [PubMed: 9904586]
20. Egawa H, Furusawa K. Langmuir 1999;15:1660–1666.
21. Reimhult E, Hook F, Kasemo B. Langmuir 2003;19:1681–1691.
22. Schonherr H, Johnson JM, Lenz P, Frank CW, Boxer SG. Langmuir 2004;20:11600–11606. [PubMed: 15595789]
23. Jass J, Tjarnhage T, Puu G. Biophysical Journal 2000;79:3153–3163. [PubMed: 11106620]
24. Richter RP, Brisson A. Langmuir 2003;19:1632–1640.
25. Seantier B, Breffa C, Felix O, Decher G. Nano Letters 2004;4:5–10.
26. Keller CA, Kasemo B. Biophysical Journal 1998;75:1397–1402. [PubMed: 9726940]
27. Kellar CA, Glasmästar K, Zhdanov VP, Kasemo B. Physical Review Letters 2000;84:5443–5446. [PubMed: 10990964]
28. Richter R, Mukhopadhyay A, Brisson A. Biophysical Journal 2003;85:3035–3047. [PubMed: 14581204]
29. Ebato H, Gentry CA, Herron JN, Muller W, Okahata Y, Ringsdorf H, Suci PA. Analytical Chemistry 1994;66:1683–1689. [PubMed: 8030782]
30. Kalb E, Frey S, Tamm LK. Biochimica Et Biophysica Acta 1992;1103:307–316. [PubMed: 1311950]
31. Richter RP, Brisson AR. Biophysical Journal 2005;88:3422–3433. [PubMed: 15731391]
32. Puu G, Gustafson I. Biochimica Et Biophysica Acta-Biomembranes 1997;1327:149–161.
33. Nissen J, Gritsch S, Wiegand G, Radler JO. European Physical Journal B 1999;10:335–344.
34. Hunter, RJ. Zeta potential in colloid science: Principles and applications. New York: Academic Press; 1981.
35. Adamson, AW.; Gast, AP. Physical chemistry of surfaces. Sixth Edition. Vol. Vol.. New York: John Wiley & Sons, Inc; 1997.
36. Vanwagenen RA, Andrade JD. Journal of Colloid and Interface Science 1980;76:305–314.
37. Frisken BJ, Asman C, Patty PJ. Langmuir 2000;16:928–933.
38. Walker SA, Kennedy MT, Zasadzinski JA. Nature 1997;387:61–64. [PubMed: 9139822]
39. Scales PJ, Grieser F, Healy TW, White LR, Chan DYC. Langmuir 1992;8:965–974.
40. Walker SL, Bhattacharjee S, Hoek EMV, Elimelech M. Langmuir 2002;18:2193–2198.
41. Seiffert S, Oppermann W. Journal of Microscopy-Oxford 2005;220:20–30.
42. Crank, J. The mathematics of diffusion. London: Oxford University Press; 1956.
43. Vanwagenen RA, Andrade JD, Hibbs JB. Journal of the Electrochemical Society 1976;123:1438–1444.
44. Kirby BJ, Hasselbrink EF. Electrophoresis 2004;25:203–213. [PubMed: 14743474]
45. Kirby BJ, Hasselbrink EF. Electrophoresis 2004;25:187–202. [PubMed: 14743473]
46. Anderson TH, Min YJ, Weirich KL, Zeng HB, Fygenson D, Israelachvili JN. Langmuir 2009;25:6997–7005. [PubMed: 19354208]
47. Tamm LK, McConnell HM. Biophysical Journal 1985;47:105–113. [PubMed: 3978184]

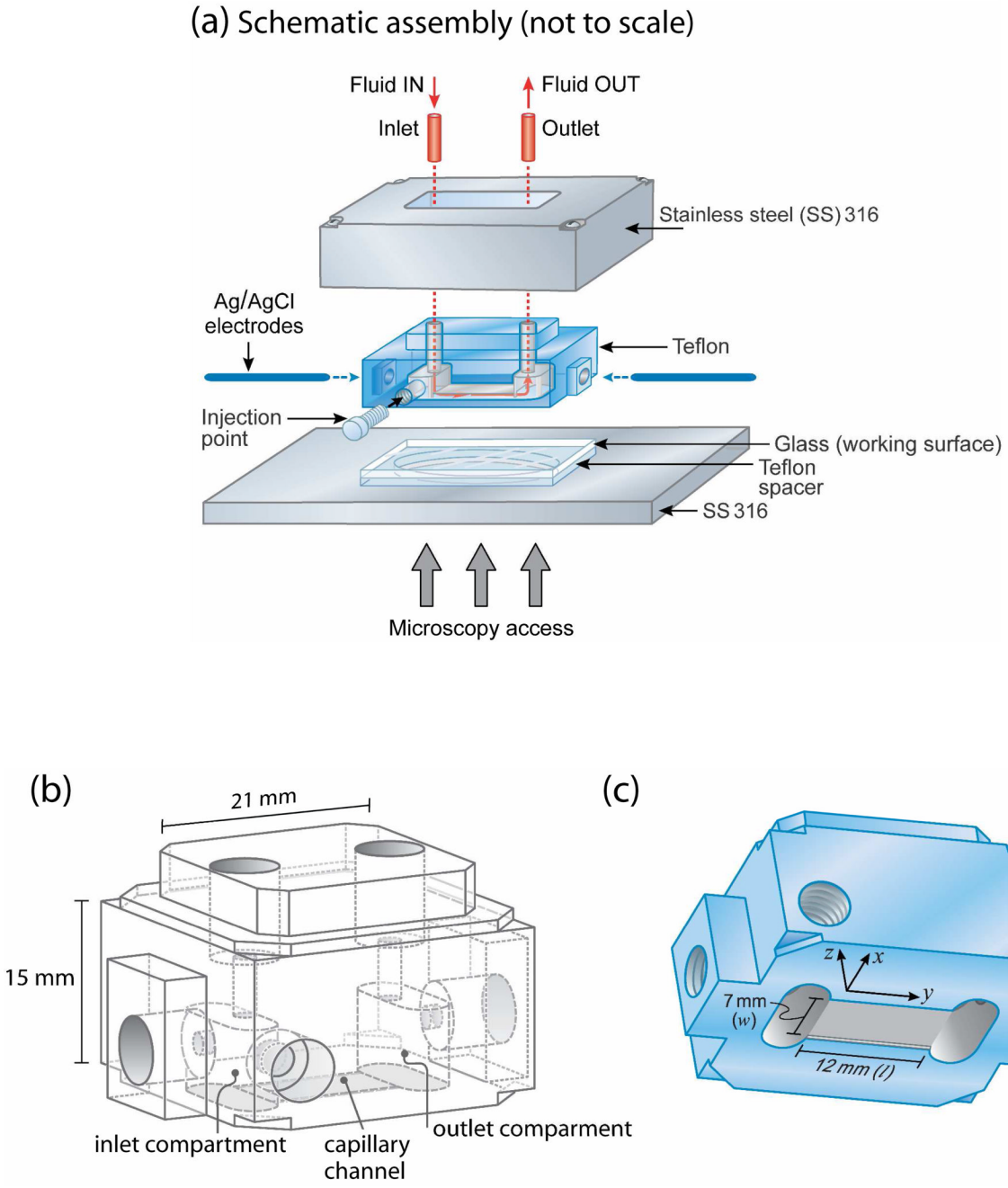

Figure 1.

(a) Miniature streaming potential apparatus (SPA) for measuring surface potentials under different solution conditions while simultaneously visualizing the state of the surfaces (e.g., adsorption of vesicles or bilayers) using confocal and/or fluorescence microscopy or FRAP. Schematic drawings of the Teflon component showing (b) its inside and (c) block cell design for parallel plate (capillary) channel of length l=12 mm (y-direction), width w=7 mm (x-direction), and height h=80 μm (z-direction). Figures (b) and (c) are drawn to scale except for the 80 μm-thick channel height which is exaggerated in (c).

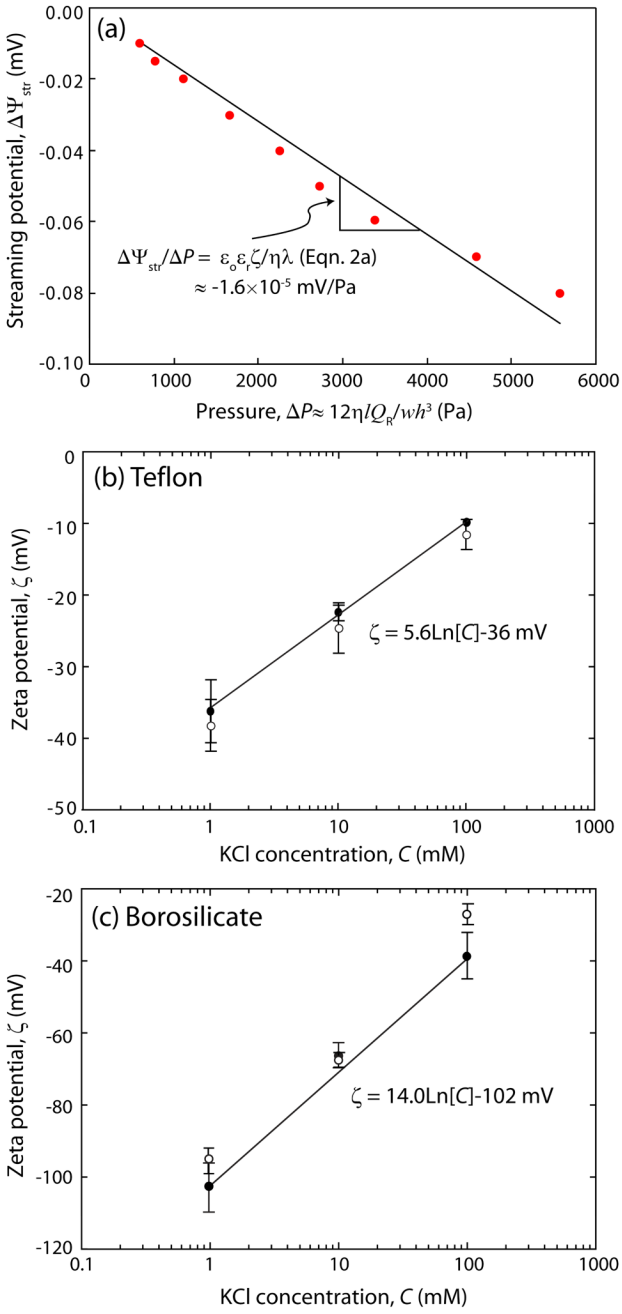

Figure 2.

(a) Variations in the measured streaming potential, $\Delta\Psi_{str}$, as a function of driving pressure, ΔP, for the capillary channel (see Fig. 1). The errors associated with various aspects of the experiments on $\Delta\Psi_{str}/\Delta P$ were estimated as ~3 %. The slope, $\Delta\Psi_{str}/\Delta P$, shown in Fig. 2(a) was used to obtain the ζ-potential based on the Helmholtz-Smoluchowski equation (Eqn. 2 (a)). Plots of ζ *vs*. *C* for a Teflon surface; calculation based on the symmetric capillary channel (Teflon *vs* Teflon, Eqn. (2a)), and a borosilicate surface based on the asymmetric capillary channel (Teflon *vs* borosilicate, Eqn. (2b)). The exponential fits are indicated by the solid lines. The open data points are previously reported ζ-potential values for Teflon[44] and borosilicate surfaces[43] at the same ionic concentrations.

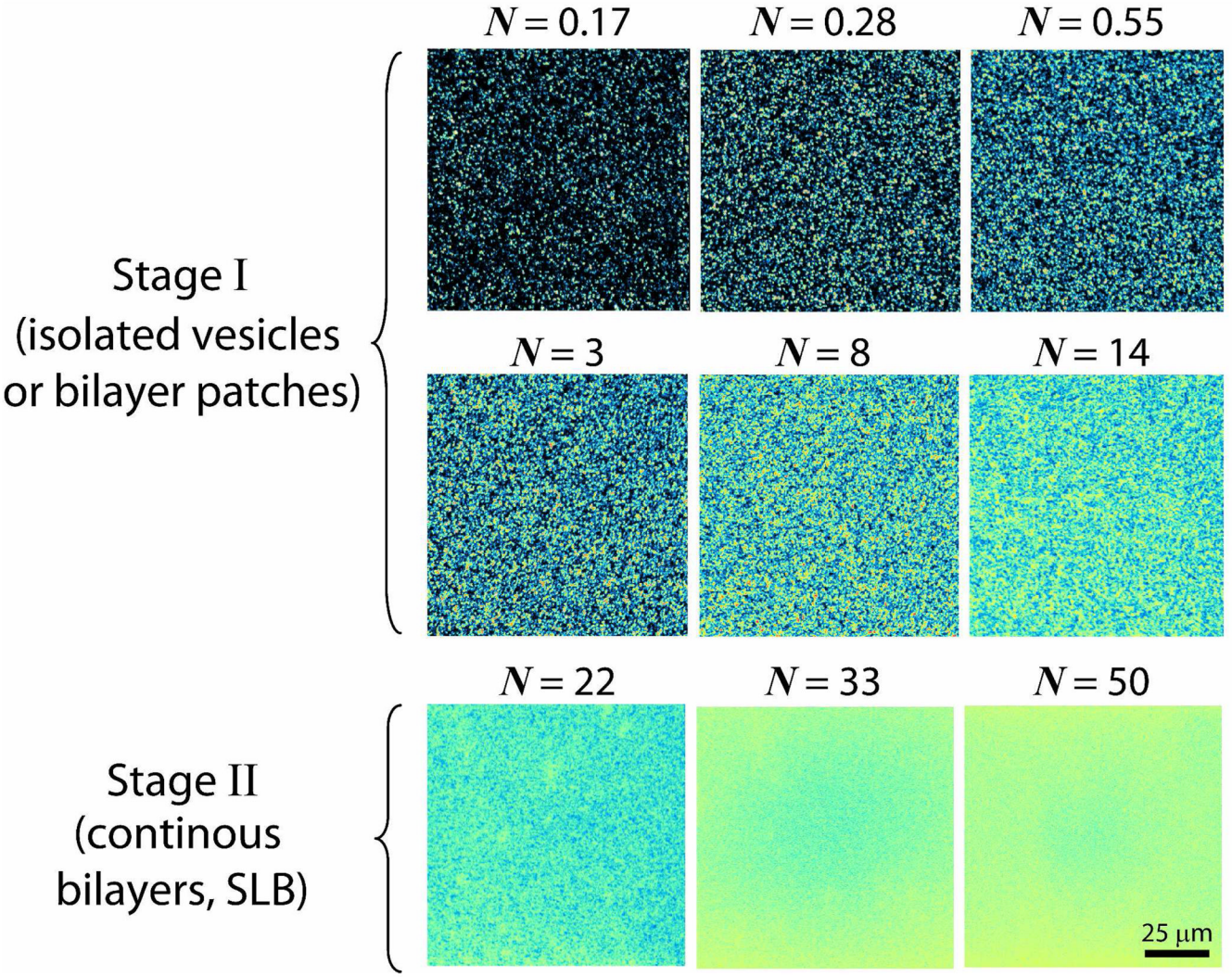

Figure 3.

Fluorescence images taken after introducing different concentrations of vesicle solutions, each containing 1 wt% of the fluorescence dye lipid TR-DHPE into the SPA chamber and incubating for 5 minutes. The number of lipid molecules injected is normalized by the number of molecules for full bilayer and monolayer coverage, this ratio being denoted by ***N***. Fluorescence images in Stage I reveal the presence of possibly two types of immobilized objects: intact vesicles and/or bilayer patches. On the other hand, defect-free bilayers appear in Stage II, indicating that (for $N \geq 22$) further addition of fresh vesicles into the SPA lead to rapid vesicle rupture and coalescence of the patchy bilayers into an SLB.

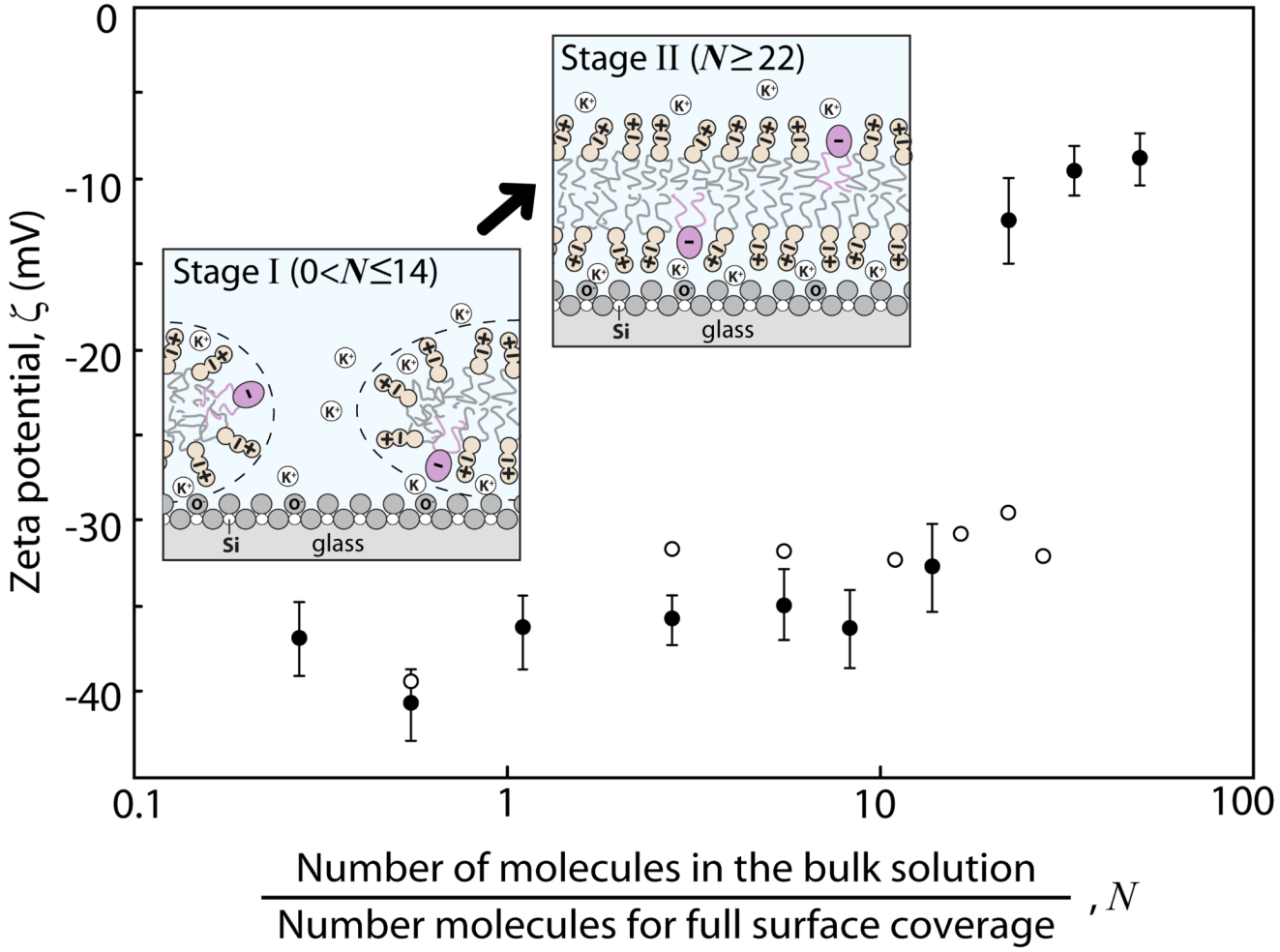

Figure 4.

Plot of ζ-potential values of the DMPC membrane-covered borosilicate surfaces as a function of ***N*** and in 100 mM KCl solution at room temperature. The different colored data points represent two independent experiments conducted under the same conditions but different injection ways: The black points represent the experiments where, for ***N***>10, ***N*** was increased in larger increments than the open circles. The two different experimental results suggest that the amount of lipid molecules added during a single injection as opposed to the same total amount added through multiple injections affects the dynamics of SLB formation. Fluorescence images and FRAP experimental data shown in Fig. 3, Fig. 5, and Fig. 6 were obtained simultaneously while measuring the ζ-potential values, shown as the black solid data points here. The first schematic in Figure 4 shows that bilayer patches form from vesicles on the negatively charged glass which is still partially exposed to the buffer solution (Stage I where the vesicle concentration in solution, $C_{vesicle}$, was varied between 0.001 and 0.05 mg/ml). The second schematic shows the glass surface fully covered by a continuous SLB but the K^+ counterions trapped between the glass and the bilayer do not completely balance with the negative charges on the surface resulting in a “non zero” ζ-potential (Stage II where $C_{vesicle}$ was varied between 0.08 and 0.1 mg/ml).

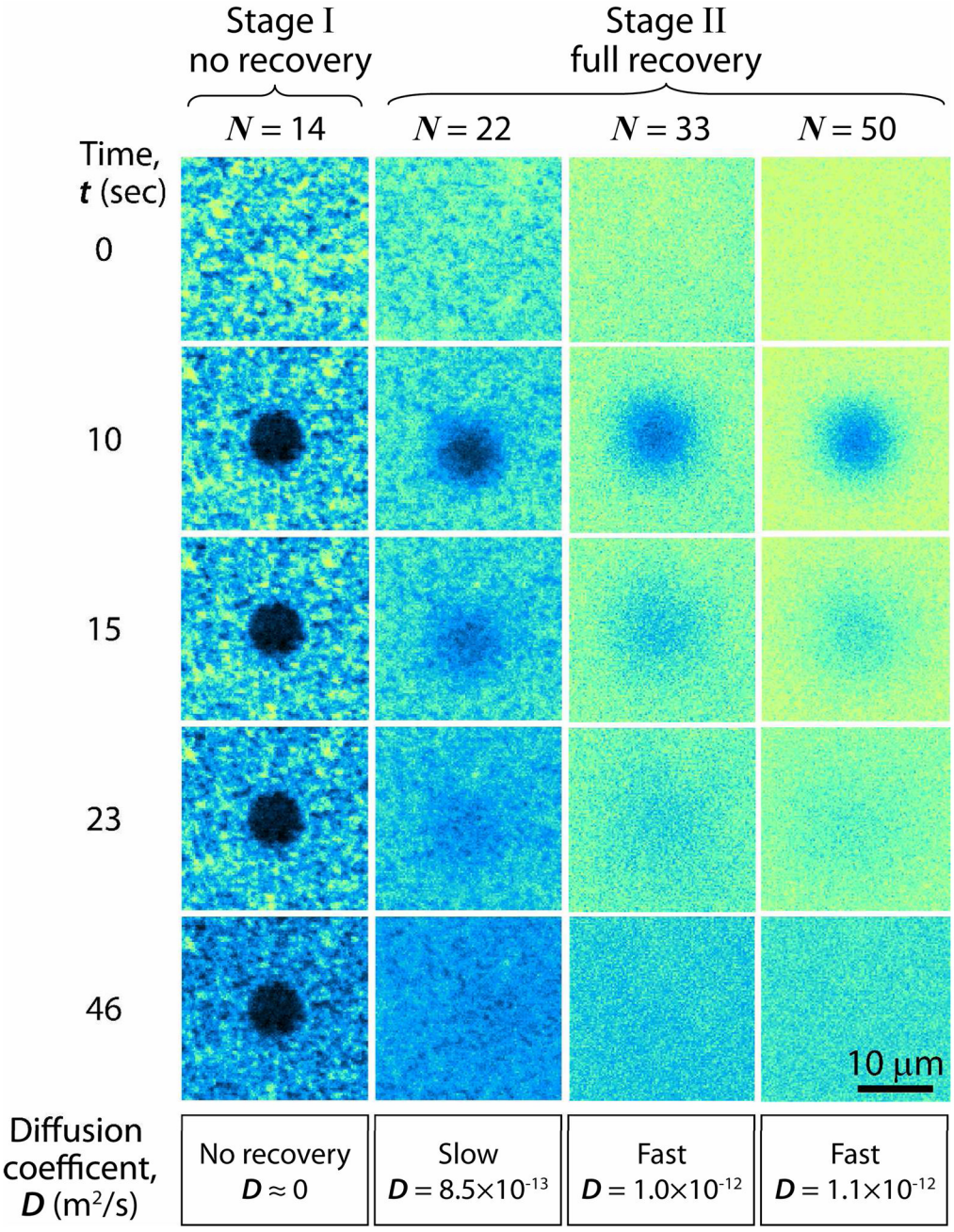

Figure 5.

FRAP images at four different DMPC vesicle concentrations, each containing 1 wt % of the fluorescent dye lipid TR-DHPE. At vesicle concentrations below ***N***=14 (Stage I) there is no recovery within 5 min, indicating that continuous bilayers do not develop on the surfaces, or do so only very slowly. In contrast, for ***N***≥22 (Stage II) there is rapid recovery after photobleaching (last three columns). The errors associated with various aspects of the experiments and analyses on D are estimated as ~2 %. The diameter of each photobleached circle is 7.5 μm.

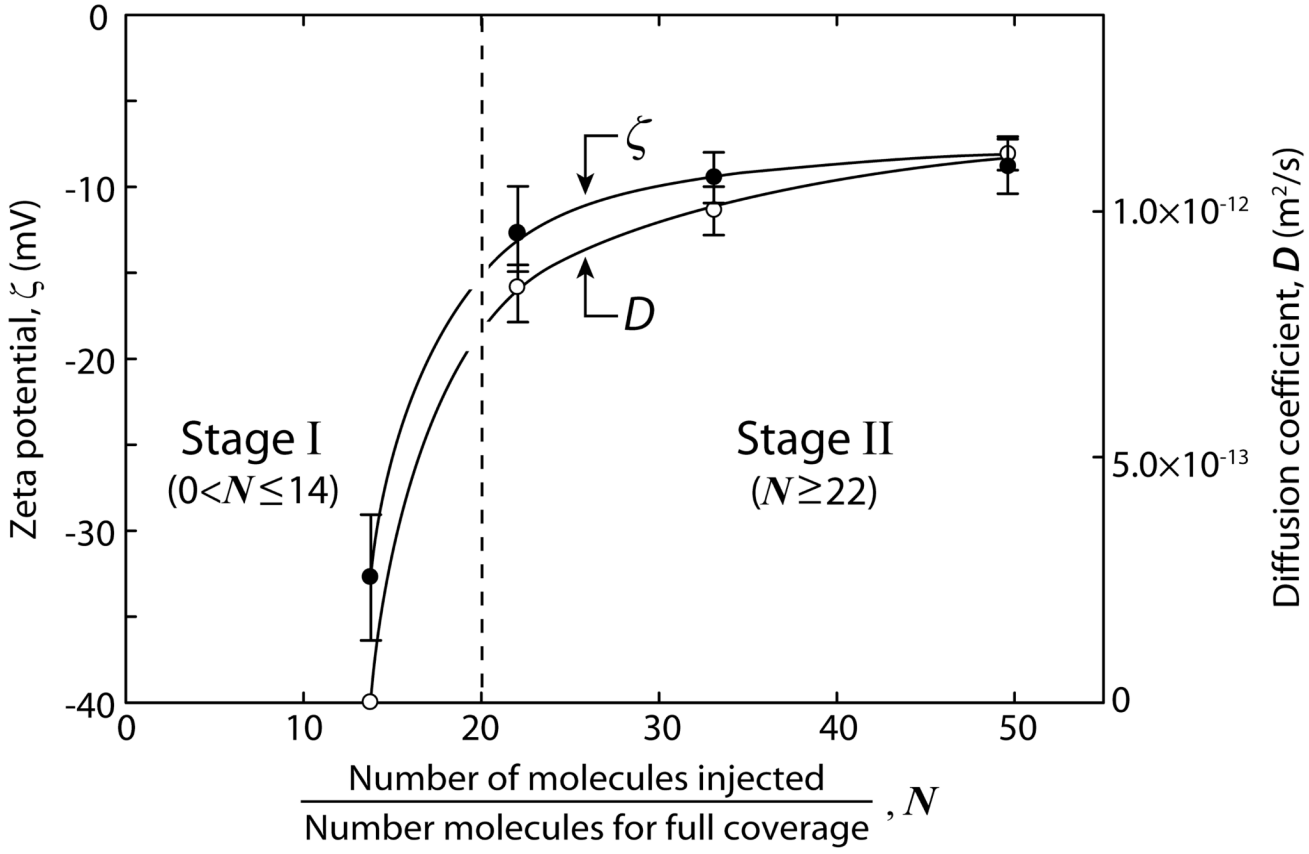

Figure 6.

Measured diffusion coefficients *D* of DMPC molecules in DMPC bilayer-covered borosilicate surfaces and corresponding ζ-potential values, both measured 10 min after introducing vesicles into the SPA chamber. Measurements were made in 100 mM KCl at room temperature. All lines shown in Figure 6 are guides to the eye.